Quantification of NO *A–X*(0, 2) laser-induced fluorescence: investigation of calibration and collisional influences in high-pressure flames

Christof Schulz, Volker Sick, Ulrich E. Meier, Johannes Heinze, and Winfried Stricker

Laser-induced-fluorescence techniques have been used successfully for quantitative two-dimensional measurements of nitric oxide. NO *A–X*(0, 2) excitation at 248 nm recently found applications in internal-combustion engines. We assess the collisional processes that influence quantification of signal intensities in terms of saturation, rotational energy transfer, and line broadening, using laminar high-pressure methane/air and *n*-heptane/air flames at pressures as high as 80 bars (8×10^6 Pa). A calibration method that is applicable in technical combustion systems based on addition of NO to the burning flame is investigated for various air/fuel ratios and pressures and yields information about the influence of NO reburn processes.

OCIS codes: 300.2530, 120.1740.

1. Introduction

Detection of nitric oxide (NO) during combustion is of particular interest because NO is a major combustion-generated pollutant. Because automotive engines play an important role in the overall production of NO and because further restrictions on release of NO into the atmosphere can be expected, measurement of NO in high-pressure processes is a subject of much interest. Laser-induced fluorescence (LIF) has been applied successfully for measurement of two-dimensional NO distributions in engine combustion. Short-wavelength excitation schemes that use 193-nm (Ref. 1) or 225-nm (Ref. 2 radiation suffer from laser attenuation when they are applied in spark-ignited engines[3] because of absorption by transient hydrocarbon species and hot CO_2.[4] Dec and Canaan showed the feasibility of NO *A–X*(0, 0) excitation under ideal conditions of Diesel combustion with a low-sooting fuel.[5] Excitation of the NO *A–X* (0, 2) band at 248 nm (Ref. 6) has been shown to give full access to the combustion chamber, even at peak pressures, in spark-ignited engines.[7–9] Practical considerations of the advantages and disadvantages of two NO A–X excitation schemes are discussed in Refs. 4, 9, and 10 and are not considered further here. The longer excitation wavelength reduces the risk of generating unwanted interfering fluorescence from hydrocarbons in fuel-rich or from O_2 Schumann–Runge emission in fuel-lean regimes.[2,3] This property can be an advantage for applications in technical combustion, particularly at elevated pressures. In any case, for quantitative interpretation of the signals obtained from LIF measurements the spectral properties that govern the excitation efficiency and the fluorescence quantum yield have to be known. Fluorescence intensities are influenced by numerous collisional processes that change the fluorescence quantum yield by quenching, influence the spectral distribution of emitted light by rotational energy transfer in the excited state, change the saturation properties and thus the linear response in excitation intensities by energy transfer in the ground state, and affect the excitation efficiency by collisional line broadening. These effects are investigated for several pressures as high as 80 bars (8×10^6 Pa) for laminar methane/air and *n*-hep-

C. Schulz is with the Physikalisch-Chemisches Institut, Universität Heidelberg, Im Neuenheimer Feld 253, 69120 Heidelberg, Germany. His e-mail address is christof.schulz@urz.uni-heidelberg.de. V. Sick is with the Department of Mechanical Engineering and Applied Mechanics, University of Michigan, Ann Arbor, Michigan 48109-2121. His e-mail address is vsick@umich.edu. U. E. Meier, J. Heinze, and W. Stricker are with the Deutsches Zentrum für Luft- und Raumfahrt, Institute of Physical Chemistry of Combustion, Pfaffenwaldring 38-40, 70569 Stuttgart, Germany, where the experimental work was performed. The e-mail address for U. E. Meier is ulrich.meier@dlr.de.

Received 6 July 1998; revised manuscript received 22 December 1998.

0003-6935/99/091434-10$15.00/0

tane/air flames. Spectroscopic studies and calibration techniques were reported previously for (0, 0) excitation; in this paper these issues are discussed for the (0, 2) transition.

Quantification of LIF measurements is usually done by calibration to account for the unknown response of the detection system. Because of the small population of $v'' = 2$ at room temperature, a source of hot NO has to be provided for calibration purposes. An *in situ* calibration method that uses NO seeded to the burn gases is studied here for a wide range of pressures and air/fuel ratios. Because NO concentrations are affected by flame chemistry, especially under fuel-rich conditions, operating conditions in which this calibration yields reliable results have to be assessed.

2. Theoretical Background

The dependence of NO LIF intensity I_{LIF} is given by the relation

$$I_{\mathrm{LIF}} \propto I_{\mathrm{Laser}} N_{\mathrm{NO}} f_B B_{ik} g_\lambda(p, T) \sum_{k,j} f_{kj} \frac{A_{kj}}{\sum_l A_{kl} + Q_k(p)}. \quad (1)$$

Relation (1) holds as long as the excitation intensity does not exceed the linear range where the fluorescence signal is proportional to the incident laser intensity I_{Laser}, and I_{LIF} depends on the number density of the excitable molecules (which is the number density N_{NO} of the species times the Boltzmann fraction f_B, which yields the population of the initial level i), the Einstein B_{ik} coefficient for absorption $i \rightarrow k$, the spectral overlap $g_\lambda(p, T)$ of the laser profile and the NO absorption spectrum, and the fluorescence quantum yield $A/(\Sigma A + Q)$, where A and Q are decay rates that are due to spontaneous emission and electronic quenching. For NO at atmospheric pressure and above, the denominator in relation (1) is dominated by electronic quenching $Q(p)$. No further depopulation processes of the excited levels such as predissociation occur for the levels under study. A variety of species-specific quenching data are available for the $v' = 0$ state,[11,12] which allow Q to be computed if the gas composition is known. The total quenching rates scale linearly with pressure. It has been shown that they are more-or-less constant for many engine conditions.[8,12]

Rotational energy transfer (RET) in the excited state causes a variety of transitions from different rotational levels that were not originally populated by laser excitation. If changes in the overall RET occur for different conditions during a measurement series, a filter function f_{kj} has to be included to account for wavelength-dependent detection efficiencies. The Einstein A and B coefficients can be calculated from spectroscopic data.[13] Pressure- and temperature-dependent broadening and shifting of the rotational fine-structure changes the overlap $g_\lambda(p, T)$ of the absorption spectrum with the laser line profile[3,14,15] and thus influences the excitation efficiency.

The temperature dependence of the population of the probed ground-state level in the range of 5%/100 K for flame temperatures that are typical for internal engine combustion (>2000 K) is described by the Boltzmann function. Therefore corrections for temperature effects are feasible when local temperatures are known from measurements[7] or calculations.[8,16]

The linear response of the LIF intensity to laser intensity is limited by saturation effects and depletion of ground-state population.[17] For data evaluation it is essential to know whether the linear assumption applies. Whereas saturation intensities of single transitions can be calculated with rate-equation models by use of the transition probabilities given by the Einstein coefficients,[18] in practical applications RET processes in the ground state and in the excited state as well as collisionally induced line-broadening effects have to be considered.

RET in the excited state populates several levels within the rotational manifold, whereas only a single transition that is resonant with the laser frequency can be depopulated by photoinduced processes. If the duration of the laser pulse is not long compared with the time necessary to reach steady state in population of the rotational manifold, pressure changes the proportion of molecules that are prone to induced emission. Furthermore, RET in the excited state may cause the spectral distribution of emitted light that is due to population of the rotational states to be different from that for the level that is directly populated by laser excitation.[18] If transition probabilities exhibited strong variations with rotational excitation, an additional pressure dependence of signal intensities would be introduced into the measurements.

Ground-state depopulation is an additional effect that has to be taken into account. RET in the ground state causes thermalization of the population of the ground-state levels on a nanosecond time scale for atmospheric-pressure conditions.[18] In high-pressure systems the increasing frequency of collisions thus extends the range of linear signal response owing to shorter fluorescence lifetimes and faster repopulation of ground-state energy levels by means of RET as long as (i) the rotational relaxation is faster than the electronic quenching[19] and (ii) the overall population of the ground-state rotational manifold is not depleted, as could occur if electronic quenching from the excited-state led preferentially to high-lying vibrational levels in the electronic ground state.

With increasing pressure, collisionally induced line broadening leads to weak excitation of a great number of different rotational levels because of the high spectral density of the NO absorption spectrum. This effect tends to wash out the saturation effect, leading to an increased range of intermediate incident laser energy densities in which neither linear dependence of LIF on laser energy nor full saturation is found.

From relation (1), semiquantitative NO concen-

trations can be obtained in the linear range if all the corrections mentioned above are applied. Quantification, however, requires the knowledge of the detection probability determined by the detection system. This value is usually obtained from calibration procedures. Different attempts at calibration have been made with Raman or Rayleigh scattered light[20,21] to investigate the imaged solid angles and the detection efficiency of optics and detectors.

However, to include transmission effects of filters used for detection it is advantageous to calibrate with the species that is to be measured. For NO LIF measurements with excitation in the A–$X(0, 0)$ band, the investigated volume can be filled with gas mixtures that contain known concentrations of NO. This calibration information could be transferred to other excitation schemes if the same excited levels were reached. The need for access to two different wavelength ranges, however, hinders the use of this method in practical applications. Direct calibration in the NO A–$X(0, 2)$ band at 248 nm is possible by doping of known quantities of NO to the burn gases, thus providing hot NO in the flame with sufficient population in the initial $v'' = 2$ level. Apart from having identical experimental parameters for the calibration, this procedure has the additional advantage of providing a chemical and physical environment that closely resembles the actual system under investigation in terms of temperature, pressure, collisional environment, saturation etc. Therefore any spectroscopic property, such as spectral distribution of the fluorescence or linewidth, affects the calibration only to the extent that it changes as a result of an interaction between the added NO and the flame. By a careful choice of the dopant levels, this interaction can be kept small or at least controllable, as we discuss in the following sections. Consequently, the extent to which added NO is affected by flame chemistry must be carefully determined. Any NO_2 that was formed from NO + O_2 in the unburned gases will instantaneously decompose at high temperatures to recycle NO.[22] Reburn reactions are known to reduce the NO concentration, especially under fuel-rich conditions.[23] On the other hand it has to be determined whether the NO dopant significantly changes the flame in terms of flame speed and temperature.

3. Experiment

Laminar, premixed methane/air and premixed prevaporized n-heptane/air flames with equivalence ratios from $\phi = 0.9$ to $\phi = 1.8$ at pressures of 1–80 bars were stabilized upon a sintered bronze plate.[24] This plate, of 8-mm diameter, was mounted in a stainless-steel housing with an inner diameter of 60 mm. The pressure could be stabilized to ± 0.03 bar. NO diluted in nitrogen (10% NO) was added to the gas mixing system to yield various NO concentrations of 0–1300 parts in 10^6 (ppm). For the measurements of saturation effects and excited-state RET the NO dopant concentration was fixed to 400 ppm. Optical access to the flame was possible via four quartz windows (Fig. 1). The beam of a frequency doubled dye laser (FWHM, 0.25 cm^{-1}; pulse length, 4–5 ns; Lumonics Hyperdye HD500 pumped at 355 nm with a Quanta Ray GCR-270 Nd:YAG laser doubled with a β-barium borate crystal in a Lumonics Hypertrac 1000 frequency doubling unit) was tuned to the NO A–$X(0, 2)$ O_{12} bandhead at 247.94 nm. It was aligned parallel to the burner surface (distance, 1.5 mm) passing the flame through the center. The pulse energy was measured with a fast photodiode calibrated against a Scientech powermeter. With a spherical telescope, a beam diameter of 0.75 mm was generated. For saturation measurements the energy density was varied from 0.5 to 85 MW/cm^2 with a dielectric attenuator (Laser Optik). For all other measurements the energy density was fixed to 15.5 MW/cm^2. Fluorescence signals were collected at right angles to the laser beam and focused with an $f = 100$ mm, $f_\# = 2$ achromatic lens onto the entrance slit of a 500-mm imaging spectrometer (Chromex 500IS), which was equipped with a 300-groove/mm grating operated in second order. For highly resolved emission spectra a 2400-groove/mm grating was used. Spectral resolutions of 10 and 3 cm^{-1}/pixel, respectively, were achieved. A narrow-band dielectric mirror (Laser Optik, highly reflecting at 248 nm, 0°, FWHM 10 nm) was used as a filter to reduce the intensity of Rayleigh Signal by 2 orders of magnitude. The dispersed fluorescence signals were detected with an intensified CCD camera (ICCD; LaVision FlameStar III). Each laser pulse yielded a complete emission spectrum with additional spatial resolution in the direction of the spectrometer slit. The signal acquired over the middle of the flame zone where temperature and concentration distributions are homogeneous[25] was averaged over 50 single shots. The signals emitted from the NO A–$X(0, 0)$, (0, 1), and (0, 3) bands as well as of the Rayleigh scattering were background corrected and included in the data evaluation.

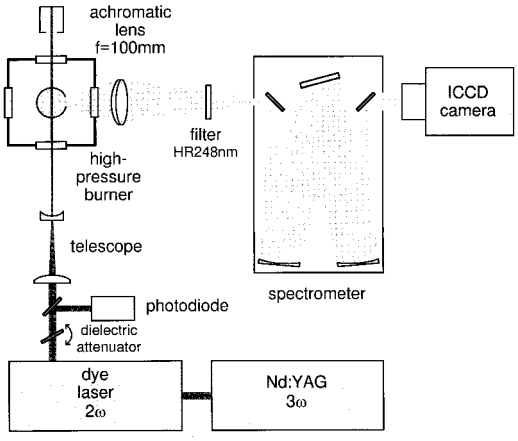

Fig. 1. Experimental setup for measurement of NO in premixed methane and n-heptane flames at 1–80 bars with various quantities of NO seeded to the burn gases.

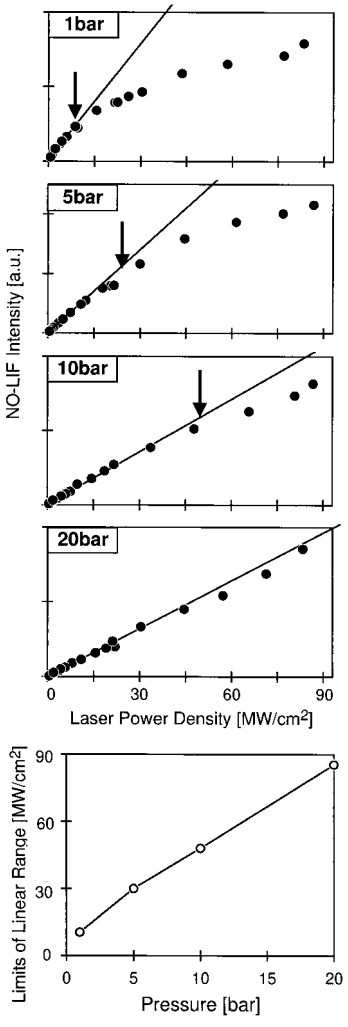

Fig. 2. Dependence of NO LIF signal intensity on laser energy density at various pressures. Bottom, limits of the linear range versus pressure. The value for 20 bars represents a lower limit only.

4. Results and Discussion

A. Limits of the Linear Regime of the NO LIF Signal

Many corrections applied when one is quantifying LIF signal intensities depend on the assumption of a linear response $I_{\mathrm{LIF}} \sim I_{\mathrm{Laser}}$. In the completely saturated regime, on the other hand, the fluorescence intensity is independent of I_{Laser}. However, the intermediate range is difficult to quantify and requires the consideration of time-dependent processes. The limits of the linear range of NO LIF on excitation at the O_{12} bandhead in the A–$X(0, 2)$ vibrational band at 247.94 nm were investigated in lean premixed flames. Signal intensities as a function of laser power densities of as much as 85 MW/cm^2 are shown for pressures of 1–20 bars (Fig. 2). For the low-pressure cases an apparent linearity can be seen only for the range of low laser power densities. The limits of this linear range are marked in the figure. Whereas at atmospheric pressure the limit is as low as 7.5 MW/cm^2 for 20 bars and higher, no deviation from the linear response could be found throughout the whole range of laser power densities accessible in the setup. Therefore only a lower limit of saturation energy densities could be obtained for 20 bars. When the limits of the linear range are plotted versus pressure (Fig. 2, bottom), a linear increase can be seen that is attributed to both the increase in quenching and the rotational-energy redistribution in the ground state, which depends on the number of collisions. In the O_{12} bandhead region several rotational lines overlap. However, inasmuch as their transition probabilities are quite similar ($A = 1.38 - 1.67 \times 10^5$ s^{-1}), no big differences in their saturation properties and thus no strong deviation from the linear dependence on pressure is expected. The laser power densities given in Fig. 2 apply to the laser system used here (FWHM, 0.25 cm^{-1}). For pressure of 5 bars and above, the line broadening is by far dominated by homogeneous broadening that is due to collisions. Thus no differences in saturation laser power densities are expected with different laser linewidths. Therefore the values given here can also be applied to measurements made with tunable excimer lasers, which usually have broader linewidths.

B. Pressure Dependence of Excitation Efficiency

Excitation efficiencies depend on the spectral overlap $g_\lambda(p, T)$ [relation (1)] of the absorption spectra and spectral shape of the laser profile, which can be calculated by use of simulated or measured absorption spectra of NO. Fluorescence excitation spectra near the NO A–$X(0, 2)$ O_{12} bandhead were recorded for various pressures and compared with simulated spectra. The pressure range shown in Ref. 3 was extended to 80 bars (Fig. 3). The pressure-dependent line-broadening coefficient 2γ was found to be $2\gamma = 0.15$ cm^{-1}/bar for flame temperature, which compares well with the data obtained from measurements in the NO A–$X(0, 0)$ band.[2,14,15] For pressures higher than 40 bars the spectral line-shape function of the NO absorption lines is expected to deviate from Lorentzian or Voigt profiles by showing an increasing asymmetry.[26] But within the experimental accuracy no significant deviations of the simulated and measured spectra were found when Voigt profiles were used for the simulation.

Figure 4 shows a comparison of measured NO LIF signal intensities for pressures from 1 to 20 bars. The flame was doped with 400-ppm NO, and the laser power density was set to 10 MW/cm^2. The data obtained from the NO A–$X(0, 1)$ emission band are corrected for broadband absorption by use of the data shown below in Subsection 4.F. The remaining decrease in signal intensity with pressure can be attributed to the decreased overlap as a result of line broadening of the rotational lines. We obtained pressure-dependent overlap factors $g_\lambda(p, T)$ by assuming a Gaussian laser line profile (FWHM, 0.25 cm^{-1}) and the spectra simulations shown in Ref. 3 as used in Fig. 3. The calculation is normalized to fit the measured value at 5 bars. From coherent anti-Stokes Raman spectroscopy measurements in the

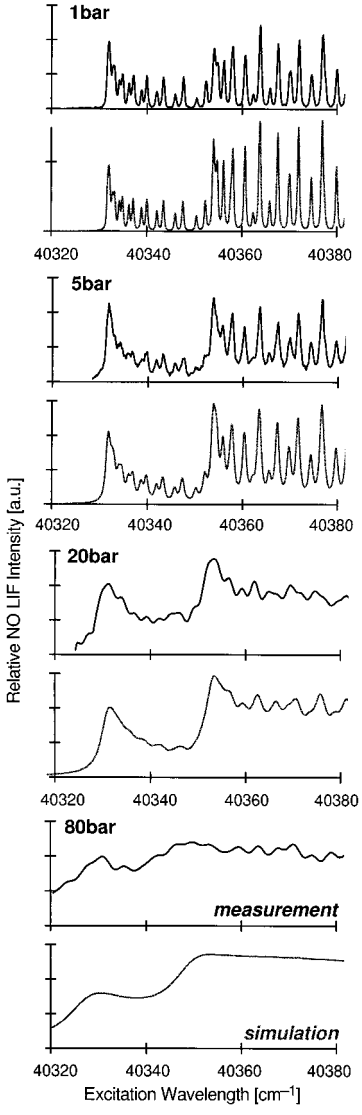

Fig. 3. Measured and calculated fluorescence excitation spectra about the NO A–$X(0, 2)$ O_{12} bandhead for four pressures.

same burner[27] it is known that from 5 to 40 bars the flame temperatures in the measurement volume decrease by 120 K because of compression of the flame and subsequent heat loss to the burner matrix. We implement this temperature change in the data shown in Fig. 4 by using the appropriate variations in ground-state populations.

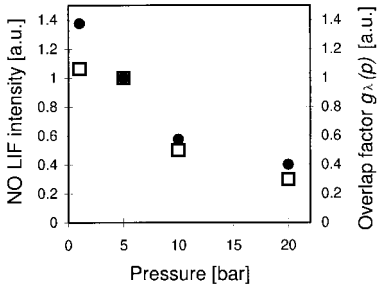

Fig. 4. Comparison of measured NO LIF intensities (on a relative scale, open squares) with calculated overlap factors $g_\lambda(p)$ (filled circles) versus pressure. Both data series are on a relative scale and are scaled to overlap at 5 bars.

Although the trend of the calculations follows the measured values, significant differences remain. The measured value at 1 bar was smaller than calculated, revealing partial saturation at the laser power density used (see Fig. 2). At 20 bars the measured LIF intensities were significantly weaker than predicted. Possible reasons for this are additional signal attenuation, possibly caused by hot CO_2 (see Ref. 28, or signal loss owing to deflection of signal light by thermal gradients in the high-pressure environment.

C. Pressure Dependence of Emission Spectra

A variation of the emission spectra with pressure can be expected as a result of collisionally induced RET in the excited state.[29] When narrow-band filters are applied for NO LIF signal detection, a variation in the spectral distribution of fluorescent light may cause a systematic pressure-dependent error. The increased number of collisions could lead to a broader distribution of the population of rotational levels within the electronically excited state. The overall effect is governed by the branching ratio RET/Q determined by the rates of collisionally induced RET and quenching. Within a typical response time τ, which depends on the rates of all depopulation processes of each individual rotational state in the excited level:

$$\tau_i = \left(\sum_k A_{ik} + \sum_k Q_{ik} + \sum_j \mathrm{RET}_{ij} \right)^{-1}, \qquad (2)$$

steady state in the population of the level i is reached.[19] With $\tau < 0.3$ ns for the cases considered here ($p > 5$ bars), steady state can be safely assumed within the laser pulse duration of 7 ns. Inasmuch as both RET and Q depend on the collision frequency and therefore on pressure, under our experimental conditions no change in branching ratios with pressure is expected. Therefore the distribution of the population within the rotational manifold is pressure independent, which prevents the occurrence of pressure effects on the spectral signature of the fluorescence signal. This also implies that changes in fluorescence cross sections with pressure because of collisionally induced population of rotational states, which exhibit different transition probabilities, are not expected.

Figure 5 shows the highly resolved emission from the (0, 1) band when the (0, 2) O_{12} bandhead is excited at pressures from 1 to 40 bars. The signal intensities are normalized to account for different excitation efficiencies, as discussed above. However, no changes in the spectral distribution of emitted light due to increased RET can be seen according to the theoretical considerations cited above. Therefore no special corrections have to be made to account for variations in emission spectra with pressure. No indication of vibrational energy transfer (VET) in the excited state was found for the operating conditions

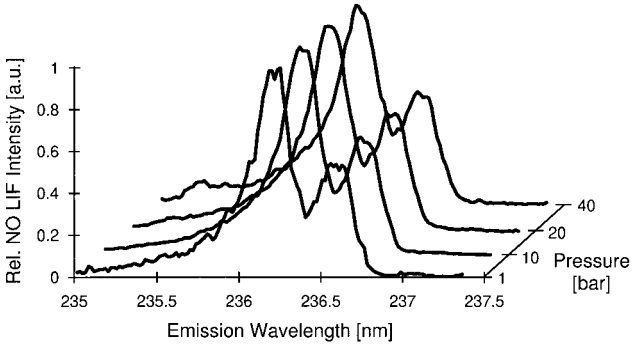

Fig. 5. Highly resolved fluorescence emission spectra from the NO A–X(0, 1) band near 236 nm on excitation at the NO A–X(0, 2) O_{12} bandhead at various pressures. Signal intensities are normalized.

under study, as we verified by using excitation-emission charts.[3] For the NO (1, 6) band at 280 nm no measurable intensity was found. The A coefficient for the (1, 6) band is $4.38 \times 10^5\ s^{-1}$,[30] which compares with $1.85 \times 10^5\ s^{-1}$ for the (0, 5) band at 285 nm. With the signal-to-noise ratio of 8 for the (0, 5) band an upper limit for VET can be estimated. Less than 5% of the laser-populated level $v' = 0$ could have been transferred to $v' = 1$ at 40 bars, resulting in a VET cross section below 0.006 nm^2.

D. Calibration by NO Addition

Calibrating semiquantitative data with a measurement by using known concentrations of the molecule under study is advantageous because in that way all effects of detection efficiency including filter transmission and collisional quenching are accounted for. Especially for two-dimensional imaging diagnostics, this fact can be of major importance. Even broadband fluorescence background from interfering species can be suppressed by use of the appropriate calibration algorithms.[31] However, when NO is excited from the second vibrational level, a source of hot NO has to be used to provide sufficient signal intensities. Doping NO to the unburned gases seems to be an excellent choice as long as the interaction between dopant and flame chemistry is small or can be quantified.

Significant reduction of NO concentration on doping into hydrogen and hydrocarbon/air flames was discussed previously. However, it has been unclear in some experiments whether catalytic effects at burner matrices have caused additional NO reduction.[32] Cattolica *et al.*[32] reported that, after reductions in NO concentrations of as much as 40%, a linear correlation between NO LIF signal and NO dopant concentration remained. These data were obtained for very high doping levels (4000–8000 ppm) in lean hydrogen/air flames. Reisel and Laurendeau[33] used NO doping to calibrate LIF measurements in hydrocarbon/air flames. They assumed that the interaction of NO with the flame is negligible at doping levels that are significantly higher than the natural NO concentrations in these flames. They cited simulation calculations that show that a reduction in doped NO concentrations of only 5% is expected in lean ($\phi = 0.9$), C_2H_4/air flames.

In a spark-ignition engine fueled with propane/air, measurements of the total NO reduction were carried out.[7,34] NO concentrations were measured simultaneously in the intake and the exhaust with a chemoluminescence probe. At dopant levels of 1000 ppm a reduction in NO concentration of only 10% in the lean flame (equivalence ratio, $\phi = 0.9$) was found. Under fuel-rich conditions ($\phi = 1.25$), reduction was increased to 40%.

Doping high concentrations of NO to the unburned gases may change the flame development and the flame temperature as well. In the same experiment no changes in engine performance were found at NO dopant levels up to 1500 ppm. Identical pressure traces to those in undoped NO showed that flame speed, heat release, and temperature are not significantly influenced by the seeding procedure. This indicates that the NO concentrations in those doped flames did not significantly alter the combustion process. At concentrations above 2000 ppm a significant reduction of peak pressures was found, indicating that the flame development was significantly changed.

When NO LIF was detected in an engine we observed that the increase in signal after 500-ppm NO was doped to the flame was significantly less than the measured increase in signal after an additional 500 ppm was added, to result in a total doping level of 1000 ppm. This result indicates that under engine conditions small amounts of doped NO are consumed more effectively, consistent with the findings in high-pressure burner measurements presented here.

The dependence of NO LIF signals on NO dopant concentration was investigated in methane/air flames at 1 and 10 bars and in prevaporized n-heptane/air at 10 bars for several air–fuel ratios. Various quantities of NO were doped to the burn gases, allowing for measurements with the addition of 0–1500 ppm of NO (10% NO in N_2). Figure 6 shows the dependence of NO LIF signal on NO dopant levels for lean ($\phi = 0.9$), stoichiometric ($\phi = 1.0$), and rich ($\phi = 1.2, 1.5, 1.8$) flames. Strong variations of the signal dependences with NO concentration can be seen. For the lean and stoichiometric flames, linear regressions were taken from the range with dopant concentrations from 400 to 1300 ppm for reasons that we elaborate below. At 1 bar the slopes for the lean, stoichiometric, and slightly rich ($\phi = 1.2$) flames are quite similar. At higher equivalence ratios the slope is significantly lower, showing a reduction of NO, which we attribute to reburn reactions. For 10 bars the onset of NO reduction (decreased slope of regression) can already be seen under slightly rich conditions, with further increases at $\phi = 1.5$ and $\phi = 1.8$. The linear trend lines for the lean and stoichiometric cases show similar slopes but different offsets. With n-heptane as the fuel, essentially the same results were obtained in lean and stoichiometric flames at 10 bars as with methane/air. For the slightly rich

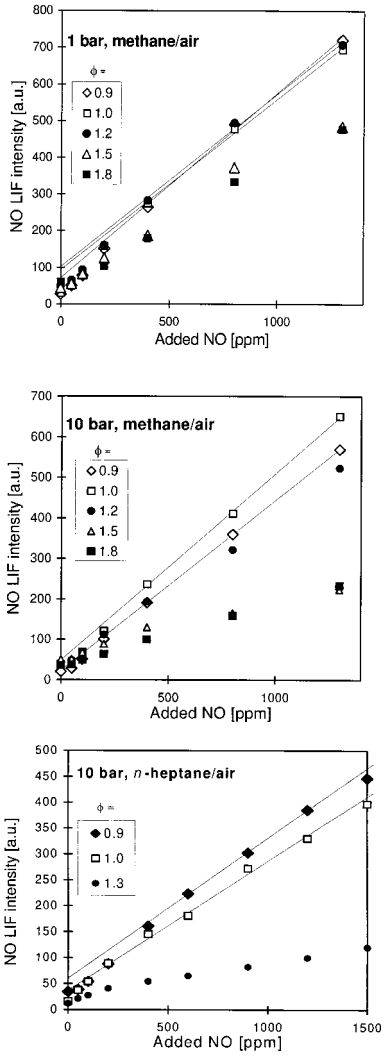

Fig. 6. NO LIF intensity versus NO dopant concentration for different pressures and fuels. Linear fits are shown for the measurements obtained for NO dopant concentrations from 500 to 1500 ppm.

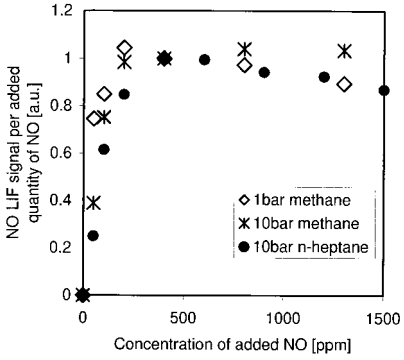

Fig. 7. Relative NO LIF signal per added quantity of NO versus NO seeding level (see text) measured in lean ($\phi = 0.9$) methane/air (1 and 10 bars) and *n*-heptane/air (10 bars) flames.

n-heptane flame ($\phi = 1.3$), however, NO seems to be reduced even more effectively than in rich methane flames with $\phi = 1.5$ and $\phi = 1.8$.

For small dopant concentrations the LIF signals are below the linear fit as described above, which indicates that there might be a potential of NO reduction that is effective and that may be related to the concentration of specific reaction partners that react effectively with NO. At higher dopant concentrations this pathway of NO destruction seems to be saturated, allowing more NO to survive and leading to a small overall reduction of NO concentrations, as observed in the engine experiments cited above. This behavior leads to a slightly delayed increase of NO LIF signal intensities with NO dopant concentration. This effect can be seen in Fig. 7, where the NO LIF signal is divided by the quantity of seeded NO. This normalized signal would have been invariant with NO concentration if no change in the interaction with flame chemistry were present. However, it can be seen clearly that strong deviations from this assumption occur at low concentrations, whereas the horizontal line is reached at higher concentrations. The slight decrease at NO dopant concentrations above 500 ppm can be attributed to cooling of the flame by dilution of the flame gases with dopant gases (0.5 vol. % at 500 ppm).

The steep slopes that are found in Fig. 7 at smaller NO concentrations, which seem to be increasingly severe at 10 bars and with burning *n*-heptane (enginelike conditions), indicate that evaluating the signal increase on addition of small quantities of NO for calibration purposes may be misleading. The nonlinear dependence of LIF signal on added NO concentration is the reason that the regression analysis in Fig. 6 was performed only over a limited NO concentration range, as we mentioned above. Using the slope of this regression for calibration eliminates background effects that are due to both initial NO destruction and natural NO formation.

E. Dependence of Collisional Quenching on Equivalence Ratio

The NO fluorescence quantum yield is dominated by collisional quenching and thus depends on the local gas composition and temperature. Calculations[35] have shown that behind the flame front the overall quenching rate is constant within 5% and is close to the rate that can be calculated for equilibrium gas compositions. Quenching in the burned gas region thus depends on air/fuel ratio and temperature. To evaluate whether the measurements shown above are influenced by changes in quenching, we calculated quenching rates for equilibrium burned gas compositions of flames at several air/fuel ratios as a function of temperature.[36] Calculations were carried out for methane/air and *n*-heptane/air flames at different equivalence ratios for 10 bars. Temperature dependences of quenching cross sections were taken from models of Paul *et al.*[11,12] The dependence of the resultant quenching rates on the air/fuel ratio and on temperature is small (Fig. 8) within the range that is relevant for our experiment.

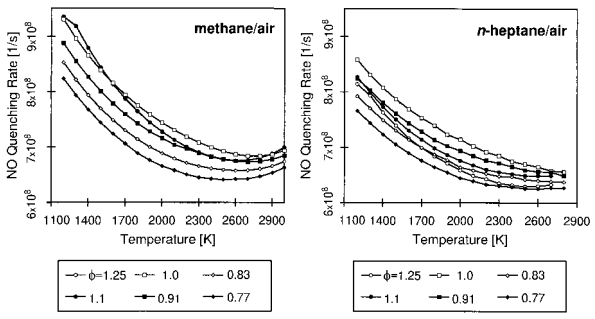

Fig. 8. NO quenching rates as a function of temperature for several air/fuel ratios in 10-bar methane/air and *n*-heptane/air flames. The rates refer to atmospheric pressure.

F. NO Fluorescence Trapping and Signal Absorption

The results presented above might be influenced additionally by fluorescence trapping, which could result in a reduced detection of NO LIF signal owing to absorption at high dopant concentrations. Because of the negligible population in the $v'' = 3$ level (<2% at flame temperatures) the LIF intensity ratio recorded from the (0, 0) and the (0, 3) bands therefore allows us to check for influences of fluorescence trapping. Figure 9 shows the ratio of signal intensities $I_{\mathrm{LIF}}[\mathrm{NO}(0,0)]/I_{\mathrm{LIF}}[\mathrm{NO}(0,3)]$ for the whole range of NO dopant concentrations. No dependence of the ratio can be seen, indicating that at NO concentrations of as much as 1300 ppm fluorescence trapping by NO is negligible. For 10 bars the ratio is reduced independently of the NO concentration, indicating broadband absorption of the short-wavelength spectral range as shown in the engine experiments,[4] probably caused by hot CO_2.[28]

A comparison of signal ratios obtained from the (0, 0) and the (0, 3) bands at 1 and 10 bars permits calculation of absorption as long as the spectral dependence of absorption coefficients are known. These data are taken from absorption measurements in engine combustion.[4] The relevant absorption coefficients for 259, 237, and 226 nm [emission wavelengths of the NO (0, 3), (0, 1), and (0, 0) bands] have been found to be $\varepsilon_{259} = 530$, $\varepsilon_{237} = 1470$, and $\varepsilon_{225} = 2500\ \mathrm{cm^2/mol}$. With the signal ratios the constant k that accounts for absorber mole fractions and path length can be calculated from Beer's law according to

$$\frac{I_{259}^{1\mathrm{bar}}/I_{226}^{1\mathrm{bar}}}{I_{259}^{p}/I_{226}^{p}} = \frac{\exp[-(\varepsilon_{259}-\varepsilon_{226})k]I_{259}^{0}/I_{226}^{0}}{\exp[-(\varepsilon_{259}-\varepsilon_{226})pk]I_{259}^{0}/I_{226}^{0}}. \quad (3)$$

When the experimentally obtained signal ratios are divided for 1 bar and $p = 10$ bars, the ratio I_{259}^{0}/I_{226}^{0} cancels. With the data shown in Fig. 9, k is calculated to be $1.51 \times 10^{-5}\ \mathrm{mol\ cm^{-2}\ bar^{-1}}$. Therefore with $\varepsilon_{237} = 1470\ \mathrm{cm^2/mol}$ absorption at 237 nm can be calculated for pressure p by

$$I_{237}^{p}/I_{237}^{0} = \exp[-p(\varepsilon_{237})k]. \quad (4)$$

The transmissions obtained are 98%, 89%, 80%, and 64% at 1, 5, 10, and 20 bars, respectively. These data are used to correct LIF intensities in Fig. 4.

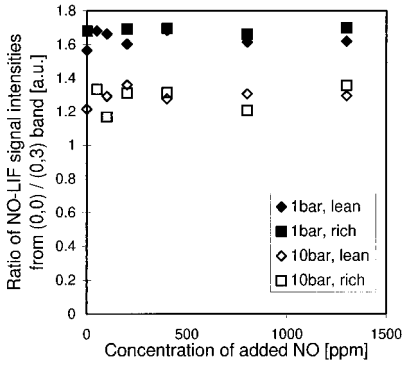

Fig. 9. Ratio of NO LIF intensities from A–$X(0, 0)$ and (0, 3) bands versus NO dopant concentration. No variation with NO concentration was found, so fluorescence trapping was excluded in the present setup (see text).

5. Conclusions

We used measurements in laminar high-pressure flames to investigate a calibration procedure and collisional influences on NO LIF to yield further information necessary for quantifying NO LIF A–$X(0, 2)$ intensities measured in technical combustion systems such as internal-combustion engines. The range of the linear fluorescence regime was investigated; with laser power densities of 15 $\mathrm{MW/cm^2}$—as are frequently used for light-sheet measurements with narrow-band excimer lasers—a pressure of 5 bars or more can be assessed without deviation from the linear dependence of signal intensities on laser power densities, thus allowing for data corrections for laser energy and pressure effects.

Simulated NO LIF spectra were compared with measurements up to 80 bars. Line-broadening coefficients were found to be $0.15\ \mathrm{cm^{-1}/bar}$ at flame temperature. The variation of NO LIF intensity with pressure was shown to be in good agreement with calculated data from spectral simulations within the error margins of the experiment. The spectral shape of the emission pattern was shown to be independent of pressure within the measured range up to 40 bars. This result proves that the effects of RET and collisional quenching cancel. No measurable influence of VET was found. The VET cross section can be estimated to be less than $0.006\ \mathrm{nm^2}$.

A calibration technique for transporting the semiquantitative data obtained after the corrections mentioned above are applied to fully quantitative values is suggested that uses NO doping of the unburned gases. We assessed the interaction of NO and flame chemistry by measuring the dependence of NO LIF signal intensity as a function of added NO concentration for various pressures and equivalence ratios in methane/air and *n*-heptane/air flames. As expected, under fuel-rich conditions the NO concentration is strongly reduced by reburn reactions, indicating that the calibration has to be performed under stoichiometric or lean conditions. Whereas at

atmospheric pressure the LIF response under slightly rich conditions is similar to that in the stoichiometric case, at 10 bars the onset of drastic reduction of NO is shifted toward stoichiometric conditions. Additionally, even under stoichiometric and lean conditions it has been shown that with small dopant levels significant deviations from the linear response are present, indicating an efficient mechanism for removing NO. The range of dopant concentrations in which this deviation was observed was found to be larger at 10 bars than at atmospheric pressure. A further increase was found with the flames fueled with *n*-heptane instead of methane. At higher dopant levels in lean flames, this pathway of NO reduction seems to be saturated, thus giving a linear increase of signal intensity with dopant concentration. Influences of fluorescence quenching and fluorescence trapping on these measurements were investigated and have been shown to be negligible under our experimental conditions.

From these findings for calibrating NO LIF measurements in enginelike environments we suggest adding NO to the lean-burning flame. Under these conditions the range of small dopant levels (below 200 ppm) should not be taken into account. Also, dopant levels above 1500 ppm can affect the combustion process itself. For the concentration range from 200 to 1500 ppm the slope of the NO LIF increase with increasing NO dopant concentration should be measured and applied when one is calibrating NO LIF signal intensities measured in an unseeded flame.

The authors acknowledge the help of Michael Decker during setting up of the experiment. This research has been funded by the Bundesministerium für Bildung, Forschung und Technologie under contracts 13N6283 (Physikalisch-Chemisches Institut, University of Heidelberg) and 13N6119 (Deutsches Zentrum für Luft- und Raumfahrt, Stuttgart).

References

1. A. M. Wodtke, L. Huwel, H. Schlüter, G. Meijer, P. Andresen, and H. Voges, "High sensitivity detection of NO in a flame using a tunable ArF excimer laser," Opt. Lett. **13,** 910–912 (1988).
2. A. O. Vyrodov, J. Heinze, M. Dillmann, U. E. Meier, and W. Stricker, "Laser-induced fluorescence thermometry and concentration measurements on NO A–X(0, 0) transitions in the exhaust gas of high pressure CH_4/air flames," Appl. Phys. B **61,** 409–414 (1995).
3. C. Schulz, V. Sick, J. Heinze, and W. Stricker, "Laser-induced fluorescence detection of nitric oxide in high-pressure flames with A–X(0, 2) excitation," Appl. Opt. **36,** 3227–3232 (1997).
4. F. Hildenbrand, C. Schulz, V. Sick, and E. Wagner, "Investigation of spatially resolved light absorption in an SI engine," Appl. Opt. **38,** 1452–1458 (1999).
5. J. E. Dec and R. E. Canaan, "PLIF imaging of NO formation in a DI Diesel engine," in *1998 SAE Congress and Exposition* (Society of Automotive Engineers, Warrendale, Pa., 1998), paper 980147.
6. C. Schulz, B. Yip, V. Sick, and J. Wolfrum, "A laser-induced fluorescence scheme for measuring nitric oxide in engines," Chem. Phys. Lett. **242,** 259–264 (1995).
7. C. Schulz, V. Sick, J. Wolfrum, V. Drewes, M. Zahn, and R. Maly "Quantitative 2D single-shot imaging of NO concentrations and temperatures in a transparent SI engine," in *Proceedings of the Twenty-Sixth International Symposium on Combustion* (Combustion Institute, Pittsburgh, Pa., 1996), pp. 2597–2604.
8. F. Hildenbrand, C. Schulz, V. Sick, G. Josefsson, I. Magnusson, Ö. Andersson, and M. Aldén, "Laserspectroscopic investigation of flow fields and NO-formation in a realistic SI engine," in *1998 SAE Congress and Exposition* (Society of Automotive Engineers, Warrendale, Pa., 1998), paper 980148.
9. M. Knapp, A. Luczak, V. Beushausen, W. Hentschel, P. Manz, and P. Andresen, "Quantitative in-cylinder NO LIF measurements with a KrF excimer laser applied to a mass-production SI engine fueled with isooctane and regular gasoline," in *1997 SAE Congress and Exposition* (Society of Automotive Engineers, Warrendale, Pa., 1997), paper 970824.
10. C. Schulz, J. Wolfrum, and V. Sick, "Comparative study of experimental and numerical NO profiles in SI combustion," in *Proceedings of the Twenty-Seventh International Symposium on Combustion* (Combustion Institute, Pittsburgh, Pa., 1998), pp. 2077–2084.
11. P. H. Paul, J. A. Gray, J. L. Durant, Jr., and J. W. Thoman, Jr., "A model for temperature-dependent collisional quenching of NO $A\ ^2\Sigma^+$," Appl. Phys. B **57,** 249–259 (1993).
12. P. H. Paul, J. A. Gray, J. L. Durant, Jr., and J. W. Thoman, Jr., "Collisional quenching corrections for laser-induced fluorescence measurements of NO $A\ ^2\Sigma^+$," AIAA J. **32,** 1670–1675 (1994).
13. P. H. Paul, "Calculation of transition frequencies and rotational line strengths in the γ-bands of nitric oxide," J. Quant. Radiat. Transfer **57,** 581–589 (1997).
14. M. D. DiRosa and R. K. Hanson, "Collisional broadening and shift of NO γ(0, 0) absorption lines by O_2, H_2O and NO at 295 K," J. Mol. Spectrosc. **164,** 97–117 (1994).
15. M. D. DiRosa and R. K. Hanson, "Collisional broadening and shift of NO γ(0, 0) absorption lines by O_2 and H_2O at high temperatures," J. Quant. Spectrosc. Radiat. Transfer **52,** 515–529 (1994).
16. G. Josefsson, I. Magnusson, F. Hildenbrand, C. Schulz, and V. Sick, "Multidimensional laser diagnostic and numerical analysis of NO formation in a gasoline engine," in *Proceedings of the Twenty-Seventh International Symposium on Combustion* (Combustion Institute, Pittsburgh, Pa., 1998), pp. 2085–2092.
17. E. W. Rothe, Y. Gu, A. Chryssostomou, P. Andresen, and F. Bormann, "Effect of laser intensity and of lower-state rotational energy transfer upon temperature measurements made with laser-induced predissociative fluorescence," Appl. Phys. B **66,** 251–258 (1998).
18. A. C. Eckbreth, *Laser Diagnostics for Combustion, Temperature and Species* (Gordon & Breach, Amsterdam, 1996).
19. G. Zizak, J. A. Lanauze, and J. D. Winefordner, "An experimental study of the excited state rotational population of OH in flames using laser induced fluorescence," Combust. Flame **65,** 203–214 (1986).
20. J. T. Salmon and N. M. Laurendeau, "Calibration of laser-saturated fluorescence measurements using Rayleigh scattering," Appl. Opt. **24,** 65–73 (1985).
21. J. Luque, G. P. Smith, and D. Crosley, "Quantitative CH determinations in low-pressure flames," in *Proceedings of the Twenty-Sixth International Symposium on Combustion* (Combustion Institute, Pittsburgh, Pa., 1996), pp. 959–966.
22. B. A. Williams and J. W. Fleming, "Comparative species concentrations in CH_4/O_2/Ar flames doped with N_2O, NO and NO_2," Combust. Flame **98,** 93–106 (1994).
23. J. Warnatz, U. Maas, and R. Dibble, *Combustion* (Springer-Verlag, Berlin, 1996).
24. H. Eberius, T. Just, T. Kick, G. Häfner, and W. Lutz, "Stabilization of premixed, laminar methane flames in the pressure

regime up to 40 bar," presented at the Joint Meeting of the German–Italian Section of the Combustion Institute, Ravello, Italy, 11–14 September 1989.
25. M. Decker, V. Sick, J. Heinze, and W. Stricker, "2D-temperature measurements in high pressure flames using LIF of molecular oxygen," in *Conference on Lasers and Electro-Optics* (*CLEO '96*), Vol. 9 of 1996 OSA Technical Digest Series (Optical Society of America, Washington, D.C., 1996), pp. 50–51.
26. A. O. Vyrodov, J. Heinze, and U. E. Meier, "Collisional broadening of spectral lines in the A–X (0, 0) system of NO by N_2, Ar, and He at elevated pressures measured by laser induced fluorescence," J. Quant. Spectrosc. Radiat. Transfer **53,** 277–287 (1995).
27. M. Woyde and W. Stricker, "The application of CARS for temperature measurements in high pressure combustion systems," Appl. Phys. B **50,** 519–525 (1990).
28. R. J. Jensen, R. D. Guettler, and J. L. Lyman, "The ultraviolet absorption spectrum of hot carbon dioxide," Chem. Phys. Lett. **277,** 356–360 (1997).
29. F. Fernandez-Allonso, G. A. Raiche, and D. R. Crosley, "Rotational energy transfer in $A\ ^2\Sigma^+$ NO in atmospheric flames and flow cells," presented at the Spring Meeting of the Western States Section of the Combustion Institute, paper 94-047 (Sandia National Laboratories, Livermore, Calif. 94551, 1994).
30. C. O. Laux and C. H. Kruger, "Arrays of radiative transition probabilities for the N_2 first and second positive, NO beta and gamma, N_2^+ first negative and O_2 Schumann–Runge band systems," J. Quant. Spectrosc. Radiat. Transfer **48,** 9–24 (1992).
31. D. D. Thomsen, F. F. Kuligowski, and N. M. Laurendeau, "Background corrections for laser-induced-fluorescence measurements of nitric oxide in lean, high-pressure, premixed methane flames," Appl. Opt. **36,** 3244–3252 (1997).
32. R. J. Cattolica, J. A. Cavalowsky, and T. G. Mataga, "Laser-fluorescence measurements of nitric oxide in low-pressure H_2/O_2/NO flames," in *Proceedings of the Twenty-Second International Symposium on Combustion* (Combustion Institute, Pittsburgh, Pa., 1988), pp. 1156–1173.
33. J. R. Reisel and N. M. Laurendeau, "Quantitative LIF measurement and modeling of nitric oxide in high-pressure C_2H_4/O_2/N_2 flames," Combust. Flame **101,** 141–152 (1995).
34. C. Schulz, "Entwicklung und Anwendung eines Laser-induzierten-Fluoreszenzverfahrens zur quantitativen Bestimmung momentaner Stickoxidverteilungen in Verbrennungsmotoren," Ph.D. dissertation (University of Heidelberg, Heidelberg, Germany, 1997).
35. A. Bräumer, V. Sick, J. Wolfrum, V. Drewes, R. R. Maly, and M. Zahn, "Quantitative two-dimensional measurements of nitric oxide and temperature in a transparent SI engine," in *1995 SAE Congress and Exposition* (Society of Automotive Engineers, Warrendale, Pa., 1995), paper 952462.
36. D. Schmidt, Institut für Technische Verbrennung, University of Stuttgart, Stuttgart, Germany (personal communication, 1998).